Tsumura-Suzuki obese diabetic mice-derived hepatic tumors closely resemble human hepatocellular carcinomas in metabolism-related genes expression and bile acid accumulation

Tetsuyuki Takahashi[1] · Ulrich Deuschle[2] · Shu Taira[3] · Takeshi Nishida[4] · Makoto Fujimoto[5] · Takao Hijikata[1] · Koichi Tsuneyama[6]

[1] Department of Anatomy and Cell Biology, Research Institute of Pharmaceutical Sciences, Faculty of Pharmacy, Musashino University, Tokyo 202-8585, Japan

[2] Phenex Pharmaceuticals AG, 69123 Heidelberg, Germany

[3] Department of Bioscience, Fukui Prefectural University, Fukui 910-1195, Japan

[4] Department of Diagnostic Pathology, Graduate School of Medical and Pharmaceutical Sciences, University of Toyama, Toyama 930-0194, Japan

[5] Department of Japanese Oriental Medicine, Graduate School of Medical and Pharmaceutical Sciences, University of Toyama, Toyama 930-0194, Japan

[6] Department of Pathology and Laboratory Medicine, Institute of Biomedical Sciences, Tokushima University Graduate School, Tokushima 770-8503, Japan

✉ Koichi Tsuneyama

e-mail: tsuneyama.koichi@tokushima-u.ac.jp

Tetsuyuki Takahashi

e-mail: te_taka@musashino-u.ac.jp

Ulrich Deuschle

e-mail:

Shu Taira

e-mail: staira@fpu.ac.jp

Takeshi Nishida

e-mail:

Makoto Fujimoto

e-mail:

Takao Hijikata

e-mail: hijikata@musashino-u.ac.jp

Abstract

Background and aims Tsumura-Suzuki obese diabetic (TSOD) is a good model of metabolic syndrome showing typical lesions found in nonalcoholic fatty liver disease and nonalcoholic steatohepatitis, and develops spontaneous hepatic tumors with a high frequency. Majority of the developing tumors overexpress glutamine synthetase (GS), which is used as a marker of hepatocellular carcinoma (HCC). The aim of this study is to assess the status of expression of metabolism-related genes and the level of bile acids in the TSOD mice-derived tumors and to determine the association with metabolic dysregulation between human HCC and TSOD mice-derived tumors.

Methods GS-positive hepatic tumors or adjacent normal tissues from71-week-old male TSOD mice were subjected to immunohistochemical staining (IHC), quantitative RT-PCR (qRT-PCR), quantitation of cholic acid and taurocolic acid.

Results We found that downregulation of the rate-limiting enzyme for betaine synthesis (BADH), at both mRNA and protein levels in GS-positive TSOD mice-derived tumors. Furthermore, the bile acid receptor FXR and the bile acid excretion pump BSEP (Abcb11) were found to be downregulated, whereas BAAT and Akr1c14, involved in primary bile acid synthesis and bile acid conjugation, were found to be upregulated at mRNA level in GS-positive TSOD mice-derived tumors. BAAT and Akr1c14 was also overexpressed at protein levels. Total cholic acid was found to be increased in GS-positive TSOD mice-derived tumors.

Conclusion Our results strongly support the significance of TSOD mice as a model of spontaneously developing HCC.

Keywords TSOD mice · HCC · Tumor metabolism · Bile acid · Spontaneous tumorigenesis model

Abbreviations

TSOD; Tsumura-Suzuki obese diabetic, GS; glutamine synthetase, HCC; hepatocellular carcinoma, IHC; immunohistochemical staining, qRT-PCR; quantitative RT-PCR

Introduction

Hepatocellular carcinoma (HCC) is the most common type of liver cancer and is one of the major causes of cancer-related deaths worldwide [1]. The curative ratio of HCC is generally low because of asymptomatic features in the initial stage and a high rate of recurrence. Molecular and clinical studies are now being increasingly carried out for developing more effective strategies for HCC therapy. The outcomes of such studies have resulted in a useful concept, the so-called molecular targeting therapy. A multikinase-inhibitor, sorafenib, that inhibits the RAF family kinases, the vascular endothelial growth factor receptors, and the platelet-derived growth factor receptor-β, has now beenapproved for treating patients with progressive HCC [2]. Following comprehensive genome and proteome studies, the metabolomic strategy has been now highlighted for understanding the systemic alteration of metabolism by several diseases, including cancer. Recent advancements in metabolome analysis methods, have now revealed the drastic changes occurring in various types of cancer tissues, including HCC [3-5]. The metabolic syndrome, defined as a group of metabolic disorders that cause cardiovascular diseases and type 2 diabetes mellitus, is also regarded as a risk factor for HCC as well as cirrhosis and infection by hepatitis B and C viruses [6].

The Tsumura-Suzuki obese diabetic (TSOD) mouse model displays typical phenotypes of metabolic syndrome, type 2 diabetes mellitus accompanied by severe obesity, glycosuria, hyperglycemia, hyperinsulinemia, and significant increase of glutamic-oxaloacetic transaminase level [7-10]. Old-aged (above 4 months of age) TSOD mice also exhibit several markers of nonalcoholic fatty liver disease (NAFLD) and nonalcoholic steatohepatitis (NASH), and finally, develop spontaneous hepatic tumors at 10 months of age [11]. Our previous studies have shown that glutamine synthetase (GS), which is one of the markers of human HCC, is also expressed in hepatic tumors of TSOD mice and that GS-positive hepatic tumors of TSOD mice and human HCC exhibit similar histopathological characteristics [12]. In this study, we assessed the status of expression of metabolism-related genes and the level of bile acid in the liver of TSOD mice to determine the association with metabolic dysregulation between human HCC and hepatic tumors of TSOD mice.

Materials and methods

TSOD mice and sample preparation

Under specific pathogen-free condition, male TSOD mice (n = 10) were maintained with MF basal diet (Oriental Yeast, Tokyo, Japan) and chlorinated tap water *ad libitum* at the Institute for Animal Reproduction (Kasumigaura, Ibaraki, Japan). The breeding procedure was performed in accordance with the animal experiment guidelines specified by the Institute for Animal Reproduction. At 71 weeks of age, mice were euthanized with excess carbon dioxide, and their livers were excised for further analyses. The excised livers were cut at macroscopic-visible tumors, and one part of the livers were fixed in 10% neutral-buffered formalin, and the remaining part was frozen with liquid nitrogen. After determining the liver samples bearing GS-positive tumors by IHC, total RNA (in tumor lesions and normal tissue) was isolated from the frozen livers using RNeasy Mini kit (Qiagen, Valencia, CA, USA). In parallel, samples were also prepared for quantitation of bile acid.

Immunohistochemical staining

Formalin-fixed tissues from TSOD mice liver were embedded in paraffin and sectioned at a thickness of 4 μm. All sections were subjected to H&E staining and IHC. Rabbit polyclonal anti-GS (Clone GS-6; dilution 1:500; Millipore, CA, USA), anti-betaine-aldehyde dehydrogenase (BADH) (1:100; Abcam, Cambridge, UK), anti-bile acid-CoA amino acid acyltransferase (BAAT) (1:200; Abcam), and anti-3α-hydroxysteroid dehydrogenase (Akr1c14) (1:200; Abcam) were used as the primary antibodies. The sections were incubated with the primary antibodies in a wet chamber for 60 min at room temperature. After rinsing with Tris-buffered saline containing 0.1% Tween 20, visualization was completed using a ChemMate ENVISION kit/horseradish peroxidase (Dako, Tokyo, Japan) following manufacturer's protocol. All sections were counterstained with Mayer's hematoxylin (Muto Pure Chemicals, Tokyo, Japan).

Gene expression analysis

The mRNA expression levels of GS, Gpc-3, choline dehydrogenase (CHD), BADH, betaine-homocysteine

methyltransferase (BHMT), carnitine O-acetyltransferase (CRAT), Δ9-desaturase (Δ-9D), Δ6-desaturase (Δ-6D), BAAT, Akr1c14, oxysterol-7α-hydroxylase (CYP7B1), cholesterol-7α-hydroxylase (CYP7A1), bile salt export pump (BSEP), and farnesoid X receptor (FXR) were assessed by qRT-PCR. Using RNAs (1 μg/sample), complementary DNAs were synthesized by SuperScript II reverse transcriptase with a random hexamer (Life Technologies, Carlsbad, CA, USA). PCR experiments were carried out using SYBR Premix EX Taq II (Takara, Shiga, Japan) and STEP One real-time PCR system (Applied Biosystems, Carlsbad, CA, USA) according to the manufacturer's protocol. The primer sequences are listed in Table 1. The relative mRNA expression levels were calculated using mouse β-actin as an internal control.

Liquid chromatography/electrospray ionization-mass spectrometry (LC/ESI-MS)

The levels of cholic acid and taurocolic acid from tumor lesion and normal tissue were quantitated using LC/ESI-MS, for which the method of sample preparation described by Hagio *et al* [13] was followed. Briefly, the tissues were homogenized in ethanol using a homogenizer. The obtained suspension was centrifuged to remove the insoluble materials. The supernatant was analyzed using LC-MS. LC was performed using an HPLC system (Infinity 1260, Agilent Technologies, Santa Clara, CA, USA) consisting of a binary pump, a degasser, an autosampler, and a thermostated column oven. An ODS column (Cosmocore, 2.1 × 100 mm, i.d., 2.6 μm, Nacalai Tesque, Kyoto, Japan) was used for separation. Solvent A was acetonitrile-water (20:80) containing 10 mM ammonium acetate. Solvent B was acetonitrile-water (80:20) containing 10 mM ammonium acetate at a flow rate of 0.4 mL/min; 0-5 min, 5% B, 5-15 min, 5%-15% B, 15-20 min, 15%-25% B; 20-22 min, 25%-75% B; and 22-24 min, 75% for wash. The MS system was used by Q-TOF MS (MaXis, Bruker Daltonik GmbH). The TOF spectra were acquired in negative ion detection mode.

Statistical analysis

All comparisons were performed using two-tailed Student's *t*-tests, and the differences were considered statistically significant when $P < 0.05$.

RESULTS

Since our previous report shows that TSNO mice, the control strain of TSOD mice, did not occur any hepatic tumors under same experimental period [11], we assessed changes of various parameters in GS-positive tumor lesions by comparing to those in adjacent normal hepatic tissues. An 80% (8/10) of mice carried one or more hepatic tumors that were visible macroscopically. No tumors were found in any other organs. We performed IHC for GS using all the tumor lesions and found that the majority of tumors (75%; 6/8) diffusely expressed GS (Fig. 1a). To validate whether GS overexpression also occurred at the mRNA level, we determined the relative mRNA level using qRT-PCR. As expected, GS mRNA levels in GS-positive tumor lesions were significantly higher than those in normal hepatic tissue. The levels of Gpc-3, known as a clinical marker of HCC, were also tested in GS-positive tumor lesions, which showed an increasing tendency, though not significant (Fig. 1b).

Tissue metabolomics using human HCC have reported decreased levels of betaine, propionylcarnitine, C18:1 free fatty acid (FFA), and C16:1 FFA and increase levels of C18:3 FFA [14]. We tested the mRNA expression of enzymes responsible for their synthesis, anabolism, or conversion, as shown in Figure 2a. BADH, which directly synthesizes betaine from betaine aldehyde, was significantly downregulated in GS-positive tumor lesions compared to that in normal tissue, whereas CDH (synthetic enzyme for betaine aldehyde) and BHMT (anabolic enzyme of betaine) were not altered. IHC for BADH was also performed using paraffin sections of GS-positive and -negative tumors. Compared to that in the adjacent normal tissue, an obvious decrease in stainability was found only in GS-positive tumors (Fig. 2b). We performed IHC for 4-hydroxy-2-nonenal (4-HNE), which is a typical product of oxidative stress of lipid. Regardless of GS positivity, all tumor lesions showed weak-positive finding, whereas normal tissue did not (data not shown). CRAT, which synthesizes propionylcarnitine from propionyl-CoA and L-carnitine, showed an increasing trend in GS-positive tumor lesions ($P = 0.11$). Δ-9D, which converts from C18:0 FFA and C16:0 FFA to C18:1 FFA and C16:1 FFA, respectively, also showed an increasing trend in GS-positive tumor lesions ($P = 0.07$). In

contrast, Δ-9D, which converts from C18:2 FFA to C18:3 FFA, showed a decreasing trend in GS-positive tumor lesions ($P = 0.09$, Fig. 2a).

We next examined the mRNA expression of the enzymes and regulators that are involved in the synthesis and excretion of primary bile acid, as shown in Figure 3. BAAT and Akr1c14, which are ultimate bile acid synthetases, showed an increasing trend in GS-positive tumor lesions ($P = 0.10$ and $P = 0.13$, respectively). Consistent with the mRNA levels, the IHC staining revealed an apparent overexpression of BAAT and Akr1c14 only in GS-positive tumors (Fig. 3a). The levels of another ultimate bile acid synthetase, CYP7B1, were not altered. CYP7A1, which plays a pivotal role in bile acid intermediate synthesis, showed a decreasing trend in GS-positive tumor lesions ($P = 0.15$, Fig. 3a). An excretory transporter of bile acid, BSEP, and its positive regulator, FXR, were apparently downregulated in GS-positive tumor lesions ($P < 0.01$, Fig. 3b). The levels of primary bile acids in GS-positive tumors and normal tissue were also measured using LC/ESI-MS. The total level of colic acid (an aggregate of all types of isomers) was significantly increased in GS-positive tumors ($P < 0.01$), whereas a moderate increase in total taurocholic acid level was found in GS-positive tumors ($P = 0.05$, Fig. 3c). However intrahepatic bile acid was found in mice bearing GS-positive tumors, typical symptoms of cholestasis (jaundice and pruritus) were not observed at the time of sacrifice (data not shown). Using IHC for α-smooth muscle actin (α-SMA), we also tested numbers of stellate cells, which have been indicated an association between obesity-Gut microbiome, bile acid-induced their senescence, and HCC progression [15], however, numbers of α-SMA-positive cells were not altered between tumor lesions and normal tissues (data not shown).

Discussion

TSOD mice are established as an inbred strain from ddY mice [7] and have used as a model of metabolic syndrome and type 2 diabetes mellitus. At an early stage of lifespan (-4 month old), typical phenomena of obesity are first shown. After then, symptoms of type 2 diabetes (hyperglycemia and hyperinsulinemia) and

pathological changes in liver (manifestations of NAFLD/NASH; namely sporadic hepatocellular ballooning, Mallory-Denk bodies, and mild lobular inflammation) begin to appear and hepatic tumors finally develop [16]. Hirayama *et al* [17] have attempted to genetic analysis of this strain and identified genetic loci to exhibit phenomena of type 2 diabetes. However, genes responsible for these pathological findings including hepatic tumorigenesis has not been identified yet. Various animal models of carcinogenesis in liver have been established using chemical carcinogens or genetic manipulation [18-21]; however, a spontaneous model of HCC is less known. The only reported model is the C3H/HeNCrj strain that develops liver tumors in 26% of mice at the age of 16-months [22]. Similar to this strain, we found that the TSOD strain develops spontaneous hepatic tumors with a high rate at 10 months of age. Our previous report also showed that the histopathological features of TSOD-derived hepatic tumors are similar to those of human HCC, including the expression pattern of the clinical marker GS [12]. To clarify whether the expression pattern of molecules responsible for the alteration of metabolism and bile acid synthesis/excretion in human HCC is altered, we conducted quantitative analyses of gene expression and primary bile acids, as well as immunohistochemical examinations. Similar to our previous report, 71-week old TSOD mice developed hepatic tumors with a high rate and with a high frequency of GS expression. Although TSOD mice are also displays typical phenotypes of NASH at 4 months of age [11, 16], we could not find any severe steatosis, fibrosis, ballooning and inflammation in non-tumor lesion of TSOD mice liver at 71-week old. Clinically, it is well known that hepatic fat loss are often found in patient with advanced NASH (called as burnt-out NASH). This similarity between TSOD mice-derived GS-positive tumors and human HCC may strengthen the utility of TSOD mice to analyze pathophysiological features during the NASH-HCC sequence. Compared with several NASH model reported previously [23-25], a remarkable point of TSOD mice is that tumorigenesis can be found under spontaneous condition with high incidence. It should be emphasized this feature if using TSOD mice as a model for NASH-HCC sequence. These GS-positive tumors also expressed Gpc-3 mRNA, which is used as another clinical marker for human HCC, with a moderately increasing trend. Unpredictably, when we attempted to detect Gpc-3 protein by IHC,

no staining patterns were found in all GS-positive- and -negative tumor lesions as well as in normal tissues (data not shown). This results suggests that post-transcriptional, translational, or post-translational regulations of Gpc-3 that affect the immunoreactivity to anti-Gpc-3 may occur in hepatic tumors from TSOD mice. To understand the biological role of Gpc-3 during tumorigenesis in this model, characteristics of Gpc-3 regulation in tumors should be clarified in future. These results suggest that the TSOD mice may be a more useful model of spontaneous HCC than are the C3H/HeNCrj mice because of the high incidence of tumorigenesis and GS and/or Gpc-3 expression levels.

Currently, it is widely known that the metabolic features of cancer tissues, including HCC, are drastically altered compared to those of normal tissues [26, 27]. Hence, we next focused on this viewpoint and assessed the expression of enzymes that are responsible for the synthesis, anabolism, or conversion of betaine, propionylcarnitine, and FFA. Our results strongly suggested that betaine levels in GS-positive tumor tissue may decrease due to the downregulation of BADH, a synthetic enzyme of betaine. Since betaine has been reported to act as an anti-oxidant and an anti-inflammatory agent [28], down-regulation of BADH may be one of the causes of tumorigenesis in the TSOD mouse liver as well as in human HCC. Results of 4-HNE level also suggests that the oxidative stress may contribute to hepatic tumorigenesis in this model, but is not likely to play a role in HCC progression. The trends of Δ-9D and Δ-6D alterations also support that consequential changes of C18:1 FFA, C16:1 FFA, and C18:3 FFA are likely to occur in TSOD mice-derived GS-positive tumors as well as in human HCC. These results suggest that a similar alteration of metabolites emerges in both TSOD mice-derived GS-positive tumors and human HCC.

Primary and secondary bile acids are indispensable digestive components; however, their excess exposure causes several diseases. In general, secondary bile acid has been believed to have carcinogenic activity [29]; however, intrahepatic bile acid (namely primary bile acid) has also been reported to be a stimulator of hepatic tumorigenesis [30, 31]. Therefore, we investigated the levels of enzymes and regulators that are involved in the synthesis and excretion of primary bile acid. As expected, the synthetic enzymes of primary bile acid, BAAT

and Akr1c14, in TSOD mice-derived GS-positive tumors were upregulated at both mRNA and protein levels. Moreover, IHC using paraffin sections from autopsy cases revealed an overexpression of BAAT and Akr1c14 only in human HCC tissues (5/5, data not shown). In contrast, CYP7A1, BSEP, and FXR were downregulated. The net levels of total cholic acid and taurocholic acid were increased, in accordance with the above-mentioned results except for CYP7A1. These data strongly suggest that multiple genes expressions, which are associated with synthesis and secretion of bile acid, alters simultaneously in TSOD mice-derived GS-positive tumors and that an excess accumulation of primary bile acids in the hepatic tissue of TSOD mice as a net result, as well as in human HCC. Especially, since BSEP and FXR are reported to be downregulated in HCC [32, 33], the same molecular basis of bile acid secretion may have occurred. Irrespective of being primary or secondary, the common biological activity of bile acid is emulsification and solubilization of cell surface components as a surfactant. This activity probably leads to cellular damage in the tissue where the overload of bile acids occurs. Our results also suggests that an accumulation of primary bile acids may play a role both in tumorigenic and tumor-progressive stage by insulting hepatic cells in this model. The fact that we did not observed any symptoms of cholestasis in mice bearing GS-positive tumors may be explained that the degree of intracellular accumulation of bile acids in this model does not reach threshold to arise macroscopic findings of cholestasis. That is, our findings, the alterations of BAAT, Akr1c14, BSEP, FXR, and primary bile acid levels, may explain why TSOD mice specifically develop hepatic tumors as well as alteration of enzyme levels in betaine- and FFA-related metabolism.

Altogether, these results suggest that the alteration of the metabolic pattern observed in human HCC also occur in GS-positive hepatic tumors of TSOD mice. Furthermore, an overloading of primary bile acid in the hepatic tissue was found. This observation indicates that the metabolic features of GS-positive hepatic tumors in TSOD mice resemble those of human HCC and that exposure of bile acid to hepatic tissue may be a trigger of tumorigenesis in TSOD mice. Our findings in this study are further evidence for using TSOD mice as a model of spontaneously occurring HCC.

Acknowledgements We thank Megimi Kume, Hitomi Umemoto, Yuki Morimoto, and Chitose Maruyama for their help and technical assistance during the histological experiments and LC/ESI-MS.

Compliance with ethical requirements

Animal study Animal care and surgical procedures were approved by the Institute for Animal Reproduction in accordance with the animal experiment guidelines outlined in the "Principle of laboratory animal care" prepared by the National Academy of Sciences and published by the National Institute of Health (NIH publication no. 85-23 revised 1985).

Conflict of interest All authors declare no conflict of interests.

Funding information This study was supported by JSPS KAKENHI Grant Numbers JP15K15098 to K. Tsuneyama and JP15K06783 to T. Takahashi.

References

1. Shen Q, Fan J, Yang XR Tan Y, Zhao W, Xu Y, et al. Serum DKK1 as a protein biomarker for the diagnosis of hepatocellular carcinoma: a large-scale, multicenter study. Lancet Oncol 2012;13(8):817-826
2. Brito AF, Abrantes AM, Tralhao JG, Botelho MF. Targeting hepatocellular carcinoma: What did we discover so far? Oncol Rev 2016;10(2):302
3. Nagrath D, Caneba C, Karedath T, Bellance N. Metabolomics for mitochondrial and cancer studies. Biochim Biophys Acta 2011;1807(6):650-663
4. Gupta S, Chawla K. Oncometabolomics in cancer research. Expert Rev Proteomics 2013;10(4):325-336
5. Wang X, Zhang A, Sun H. Power of metabolomics in diagnosis and biomarker discovery of hepatocellular carcinoma. Hepatology 2013;57(5):2072-2077

6. Mendonça FM, de Sousa FR, Barbosa AL, Martins SC, Araújo RL, Soares R, et al. Metabolic syndrome and risk of cancer: which link? Metabolism 2015;64(2):182-189

7. Suzuki W, Iizuka S, Tabuchi M, Funo S, Yanagisawa T, Kimura M, et al. A new mouse model of spontaneous diabetes derived from ddY strain. Exp Anim 1999;48(3):181-189

8. Miura T, Suzuki W, Ishihara E, Arai I, Ishida H, Seino Y, et al. Impairment of insulin-stimulated GLUT4 translocation in skeletal muscle and adipose tissue in the Tsumura Suzuki obese diabetic mouse: a new genetic animal model of type 2 diabetes. Eur J Endocrinol 2001;145(6):785-790

9. Takahashi A, Tabuchi M, Suzuki W, Iizuka S, Nagata M, Ikeya Y, et al. Insulin resistance and low sympathetic nerve activity in the Tsumura Suzuki obese diabetic mouse: a new model of spontaneous type 2 diabetes mellitus and obesity. Metabolism 2006;55(12):1664-1669

10. Akase T, Shimada T, Harasawa Y, Akase T, Ikeya Y, Nagai E, et al. Preventive effects of Salacia reticulata on obesity and metabolic disoders in TSOD mice. Evid Based Complement Alternat Med 2011;2011:484590

11. Nishida T, Tsuneyama K, Fujimoto M, Nomoto K, Hayashi S, Miwa S, et al. Spontaneous onset of nonalcoholic steatohepatitis and hepatocellular carcinoma in a mouse model of metabolic syndrome. Lab Invest 2013;93(2):230-241

12. Takahashi T, Nishida T, Baba H, Hatta H, Imura J, Sutoh M, et al. Histopathological characteristics of glutamine synthetase-positive hepatic tumor lesions in a mouse model of spontaneous metabolic syndrome (TSOD mouse). Mol Clin Oncol 2016;5(2):267-270

13. Hagio M, Matsumoto M, Fukushima M, Hara H, Ishizuka S. Improved analysis of bile acids in tissues and intestinal contents of rats using LC/ESI-MS. J Lipid Res 2009;50(1):173-180

14. Huang Q, Tan Y, Yin P, Ye G, Gao P, Lu X, et al. Metabolic characterization of hepatocellular carcinoma using nontargeted tissue metabolomics. Cancer Res 2013;73(16):4992-5002

15. Yoshimoto S, Loo TM, Atarashi K, Kanda H, Sato S, Oyadomari S, et al. Obesity-induced gut microbial metabolite promotes liver cancer through senescence secretome. Nature 2013;499(7456):97-101

16. Tsuneyama K, Nishitsuji K, Matsumoto M, Kobayashi T, Morimoto Y, Tsunematsu T, et al. Animal models for analyzing metabolic syndrome-associated liver disease. Pathol Int 2017;67(11):439-546

17. Hirayama I, Yi Z, Izumi S, Arai I, Suzuki W, Nagamachi Y, et al. Genetic analysis of obese diabetes in the TSOD mouse. Diabetes 1999;48(5):1183-1191

18. Vesselinovitch SD, Mihailovich N, Rao KV. Morphology and metastatic nature of induced hepatic nodular lesions in C57BL x C3H F1 mice. Cancer Res 1978;38(7):2003-2010

19. McGlynn KA, Hunter K, LeVoyer T, Roush J, Wise P, Michielli RA, et al. Susceptibility to aflatoxin B1-related primary hepatocellular carcinoma in mice and humans. Cancer Res 2003;63(15):4594-4601

20. Ullrich SJ, Zeng ZZ, Jay G. Transgenic mouse models of human gastric and hepatic carcinomas. Semin Cancer Biol 1994;5(1):61-68

21. Pikarsky E, Porat RM, Stein I, Abramovitch R, Amit S, Kasem S, et al. NF-kappaB functions as a tumour promoter in inflammation-associated cancer. Nature 2004;431(7007):461-466

22. Kushida H, Wakabayashi K, Suzuki M, Takahashi S, Imaida K, Sugimura T, et al. Suppression of spontaneous hepatocellular carcinoma development in C3H/HeNCrj mice by the lipophilic ascorbic acid, 2-O-octadecylascorbic acid (CV-3611). Carcinogenesis 1992;13(6):913-915

23. Nakanishi Y, Tsuneyama K, Fujimoto M, Salunga TL, Nomoto K, An JL, et al. Monosodium glutamate (MSG): a villain and promoter of liver inflammation and dysplasia. J Autoimmun 2008;30(1-2):42-50

24. Fujii M, Shibazaki Y, Wakamatsu K, Honda Y, Kawauchi Y, Suzuki K, et al. A murine model for non-alcoholic steatohepatitis showing evidence of association between diabetes and hepatocellular carcinoma. Med Mol Morphol 2013;46(3):141-152

25. Akiyama K, Warabi E, Okada K, Yanagawa T, Ishii T, Kose K, et al. Deletion of both p62 and Nrf2 spontaneously results in the development of nonalcoholic steatohepatitis. Exp Anim 2017;in press

26. Spratlin JL, Serkova NJ, Eckhardt SG. Clinical applications of metabolomics in oncology: a review. Clin Cancer Res 2009;15(2):431-440

27. Holmes E, Wijeyesekera A, Taylor-Robinson SD, Nicholson JK. The promise of metabolic phenotyping in gastroenterology and hepatology. Nat Rev Gastroenterol Hepatol 2015;12(8):458-471.

28. Bingûi I, Aydin AF, Başaran-Kūcűkgergin C, Doğan-Ekici I, Çoban J, Doğru-Abbasoğlu S, et al. High-fat diet plus carbon tetrachloride-induced liver fibrosis is alleviated by betaine treatment in rats. Int Immunopharmacol 2016;39:199-207

29. Baptissart M, Vega A, Magdasy S, Caira F, Baron S, Lobaccaro JM, et al. Bile acids: from digestion to cancers. Biochimie 2013;95(3):504-517

30. Lozano E, Sanchez-Vicente L, Monte MJ, Herraez E, Briz O, Banales JM, et al. Cocarcinogenic effects of intrahepatic bile acid accumulation in cholangiocarcinoma development. Mol Cancer Res 2014;12(1):91-100

31. Zhang W, Zhou L, Yin P, Wang J, Lu X, Wang X, et al. A weighted relative difference accumulation algorithm for dynamic metabolomics data: long-term elevated bile acids are risk factors for hepatocellular carcinoma. Sci Rep 2015;5:8984

32. Zollner G, Wagner M, Fickert P, Silbert D, Fuchsbichler A, Zatloukal K, et al. Hepatobiliary transporter expression in human hepatocellular carcinoma. Liver Int 2005;25(2):367-379

33. Wolfe A, Thomas A, Edwards G, Jaseja R, Guo GL, Apte U. Increased activation of the Wnt/β-catenin pathway in spontaneous hepatocellular carcinoma observed in farnesoid X receptor knockout mice. J Pharmacol Exp Ther 2011;338(1):12-21

Figure Legends

Fig. 1 Hepatic tumors in TSOD mice. **a** Representative images of GS-positive and –negative tumor lesions in 71-week old male TSOD mice. Dotted lines in the H&E section are borderlines between normal and tumor

lesions. *T*, tumor lesion. **b** The levels of GS and Gpc-3 in GS-positive tumors and adjacent normal liver tissue were determined using qRT-PCR. The relative expression levels were calculated using values of β-actin qRT-PCR as an internal standard. *Columns*, mean values (n = 6); *bars*, SD. * P <0.05 by Student's *t*-test (compared to values in normal tissue).

Fig. 2 mRNA and protein expression of enzymes that are responsible for the synthesis, anabolism, or conversion of betaine, propionylcarnitine, and FFA in GS-positive TSOD mice-derived hepatic tumors. **a** The levels of CHD, BADH, BHMT, CRAT, Δ-9D, and Δ-6D in GS-positive tumors and adjacent normal liver tissue were determined using qRT-PCR. The relative expression levels were calculated using values of β-actin qRT-PCR as an internal standard. *Columns*, mean values (n = 6); *bars*, SD. **b** GS-positive and -negative tumors, including the adjacent normal tissue, were subjected to IHC for BADH. *N*, normal tissue; *T*, tumor lesion. * P <0.05 by Student's *t*-test (compared to values in normal tissue).

Fig. 3 mRNA and protein expression of enzymes that are involved in the synthesis and excretion of primary bile acid in GS-positive TSOD mice-derived hepatic tumors. **a** The levels of BAAT, Akr1c14, CYP7A1, CYP7B1, and CYP8B1 in GS-positive tumors and adjacent normal liver tissue were determined using qRT-PCR. The relative expression levels were calculated using values of β-actin qRT-PCR as an internal standard. *Columns*, mean values (n = 6); *bars*, SD. In parallel, GS-positive and -negative tumors, including the adjacent normal tissue, were subjected to IHC for BAAT and Akr1c14. *N*, normal tissue; *T*, tumor lesion. **b** The levels of BSEP and FXR in GS-positive tumors and adjacent normal liver tissue were determined using qRT-PCR. The relative expression levels were calculated using values of β-actin qRT-PCR as an internal standard. *Columns*, mean values (n = 6); *bars*, SD. **c** Intrahepatic levels of total CA and total TCA in GS-positive tumors and adjacent normal liver tissue were determined using LC/ESI-MS. *Columns*, mean values (n = 4-5); *bars*, SD. ** P <0.01 by Student's *t*-test (compared to values in normal tissue).

Figure 1

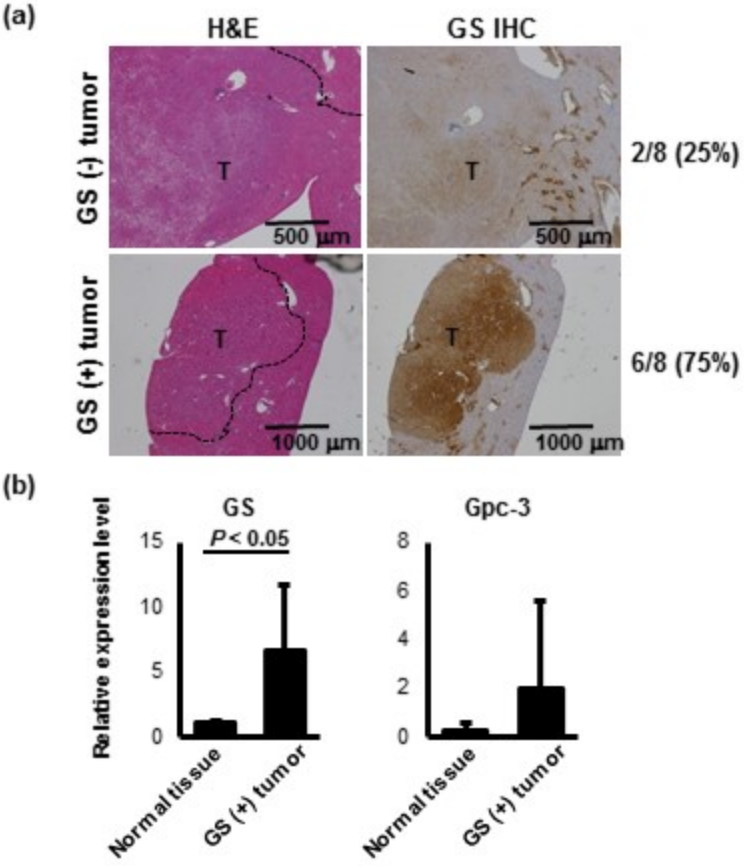
(a)
H&E
GS IHC
GS (-) tumor
GS (+) tumor
T
500 μm
1000 μm
2/8 (25%)
6/8 (75%)
(b)
GS
Gpc-3
P < 0.05
Relative expression level
15
10
5
0
8
6
4
2
0
Normal tissue
GS (+) tumor

Figure 2

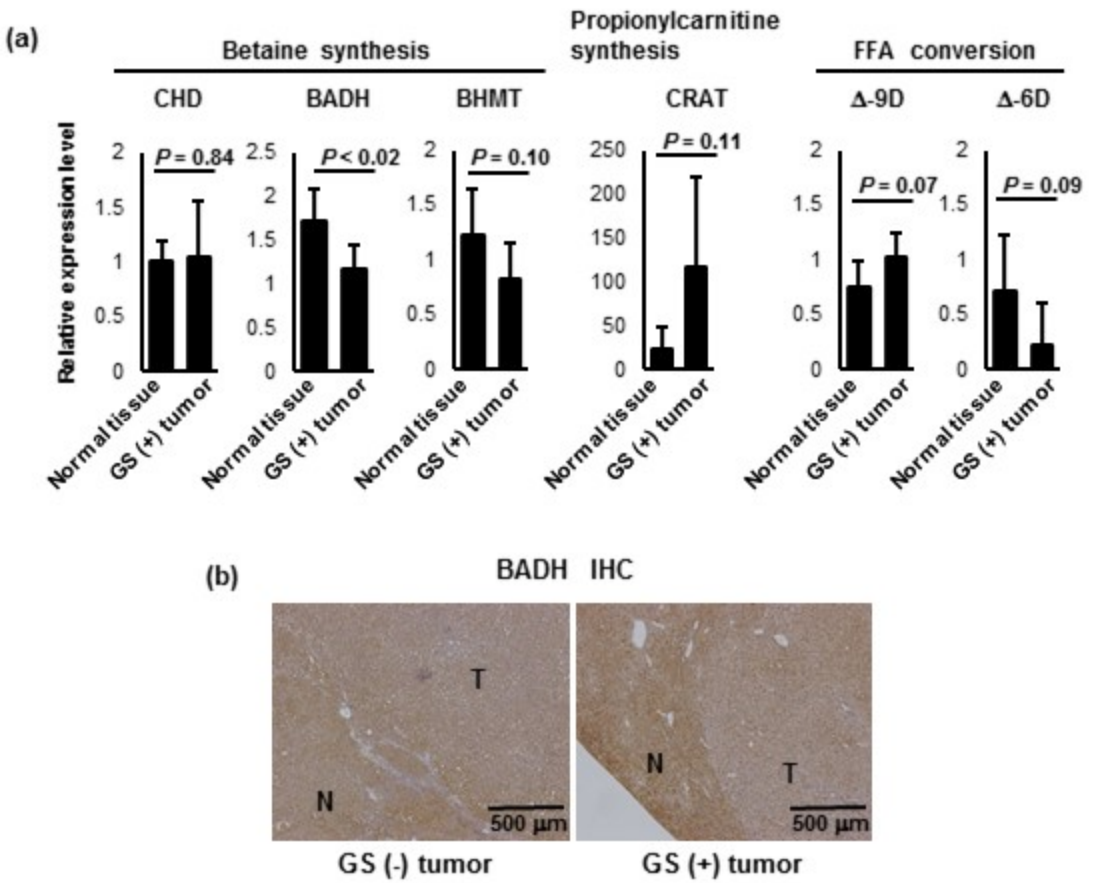
(a)
Betaine synthesis
Propionylcarnitine synthesis
FFA conversion
CHD
BADH
BHMT
CRAT
Δ-9D
Δ-6D
Relative expression level
P = 0.84
P < 0.02
P = 0.10
P = 0.11
P = 0.07
P = 0.09
Normal tissue
GS (+) tumor
(b)
BADH IHC
T
N
500 μm
GS (-) tumor
GS (+) tumor

Figure 3

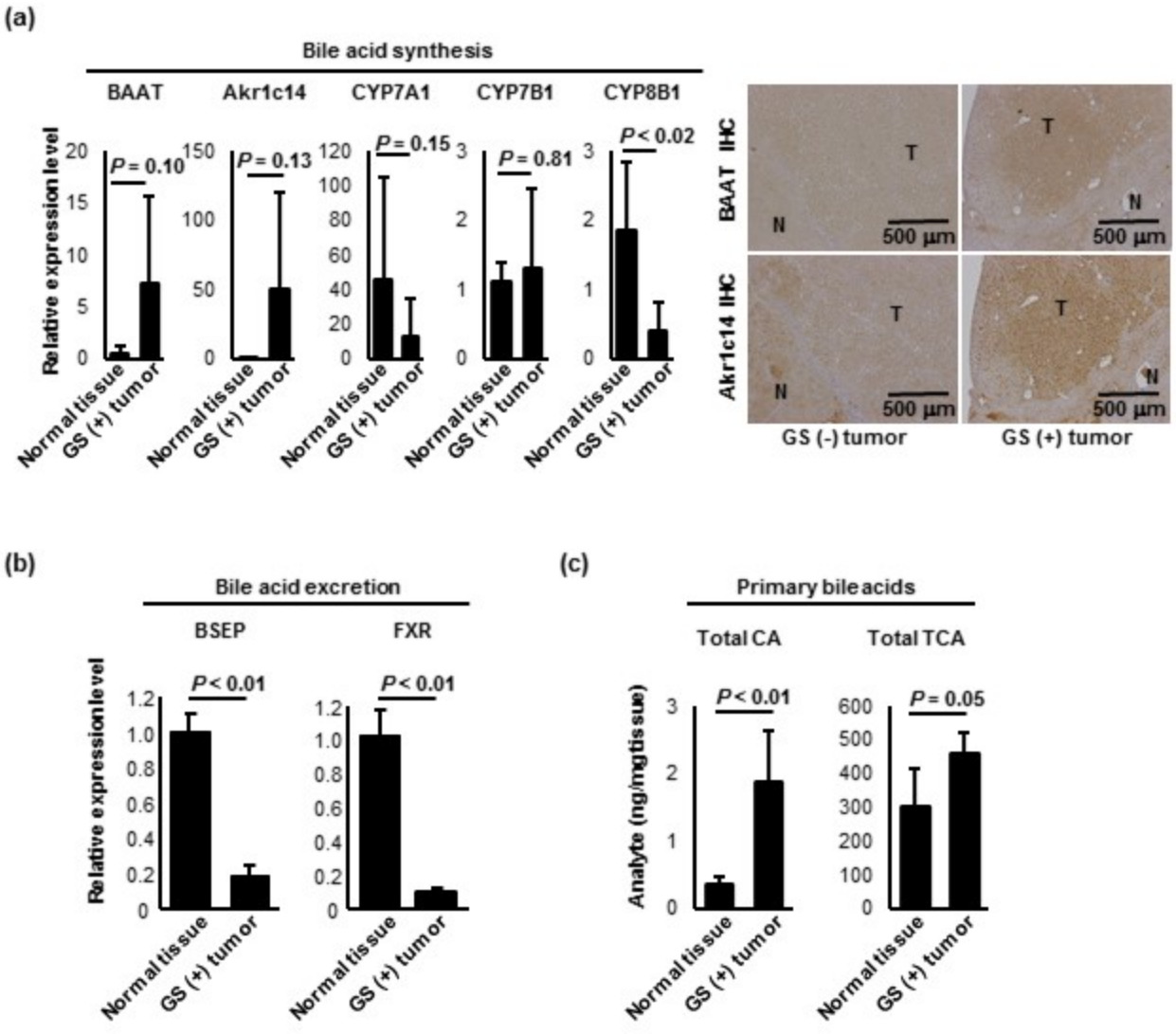
(a)
Bile acid synthesis
BAAT
Akr1c14
CYP7A1
CYP7B1
CYP8B1
Relative expression level
P = 0.10
P = 0.13
P = 0.15
P = 0.81
P < 0.02
Normal tissue
GS (+) tumor
BAAT IHC
Akr1c14 IHC
T
N
500 μm
GS (-) tumor
GS (+) tumor
(b)
Bile acid excretion
BSEP
FXR
P < 0.01
P < 0.01
(c)
Primary bile acids
Total CA
Total TCA
Analyte (ng/mg tissue)
P < 0.01
P = 0.05

Table 1 Primer sequences for qRT-PCR

Target	Forward (5' to 3')	Reverse (5' to 3')
mGS	AACACCTTCCACCATGGCCA	TGTCGCTGTTGGAGCCTTCA
mGpc3	AGGACTGTGGCCGTATGCTC	TGCCTCCGTTCTTCTGCACA
mCHD	GCGGCTCCTCATCCCTCAAT	TGAAGCGGGTGGTTGGTCTT
mBADH	AACCCACCATTGTGACCGGT	CGTTCACGATGCCACAGTCG
mBHMT	GCTACCATGTGCATTGGGCC	TGTTTGCCACAGTCAGGGGT
mCRAT	TCTCTAGCAAGGCCCCAACG	TTTTGGCCTGGCTGTGGAGA
mΔ-9D	GCAAACACCCGGCTGTCAAA	ATAGAGATGCGCGGCACTGT
mΔ-6D	CGGGACTGGCTGGATTCCTA	CCATACTCAAGGGGCTGCCA
mBAAT	CACACCACGTTCCTGAGGGT	ACCTCACCCACTTCACTGGC
mAkr1c14	CTTCAGGCAGCTGGAGACGA	TCAGGACCACAATTCCACGCT
mCYP7A1	GGAAAGGCTGGCTGAGAGCT	TGGCATTCCCTCCAGAGCTG
mCYP7B1	CCCCCAAATGCAACCGCTAC	AGGCACAGCTTTCTGGCAGA
mCYP8B1	TGAAGGCTGTGCGTGAGGAA	AGCCACCTTATCTCCGCGAC
mBSEP	CCTCATACGGAAACCCAAGATC	CCTCATACGGAAACCCAAGATC
mFXR	GGACGGGATGAGTGTGAAG	TGAACTTGAGGAAACGGGAC
mβ-actin	GGCTCCTAGCACCATGAAGA	GTACTTGCGCTCAGGAGGAG